Supporting Information

Targeting multiple effector pathways in pancreatic ductal adenocarcinoma with a G-quadruplex-binding small molecule

Chiara Marchetti[†], Katherine G. Zyner[‡], Stephan A. Ohnmacht[†], Mathew Robson[§], Shozeb M. Haider[†], Jennifer P. Morton[ǁ,¶], Giovanni Marsico[‡], Tam Vo[#], Sarah Laughlin-Toth[#], Ahmed A. Ahmed[†], Gloria Di Vita[†], Ingrida Pazitna[†], Mekala Gunaratnam[†], Rachael J. Besser[†], Ana Catarina Gomes Andrade[†], Seckou Diocou[¥], Jeremy A. Pike[‡,Δ], David Tannahill[‡], R. Barbara Pedley[7], T.R. Jeffry Evans[ǁ,¶], W. David Wilson[#], Shankar Balasubramanian[‡,Φ,π] and Stephen Neidle[†]*

[†]UCL School of Pharmacy, University College London, 29-39 Brunswick Square, London WC1N 1AX, UK.

[‡]Cancer Research UK Cambridge Research Institute, Li Ka Shing Centre, Robinson Way, Cambridge CB2 0RE, UK.

[§]Cancer Research UK Cancer Centre, UCL Cancer Institute, University College London, London WC1E 6BT, UK.

[ǁ]Cancer Research UK Beatson Institute, Garscube Estate, Switchback Rd, Glasgow G61 1BD UK.

[¶]Institute of Cancer Sciences, University of Glasgow, Glasgow G12 8QQ.

[#]Department of Chemistry and Center for Biotechnology and Drug Design, Georgia State University, Atlanta, Georgia 30303-3083, USA.

[¥]UCL Cancer Institute, University College London, London WC1E 6BT, UK.

[Δ]Now at: Centre of Membrane Proteins and Receptors, University of Birmingham, Birmingham, B15 2TT, UK.

[Φ]Department of Chemistry, University of Cambridge, Cambridge CB2 1EW, UK.

[π]The School of Clinical Medicine, University of Cambridge, Cambridge, CB2 0SP, U.K.

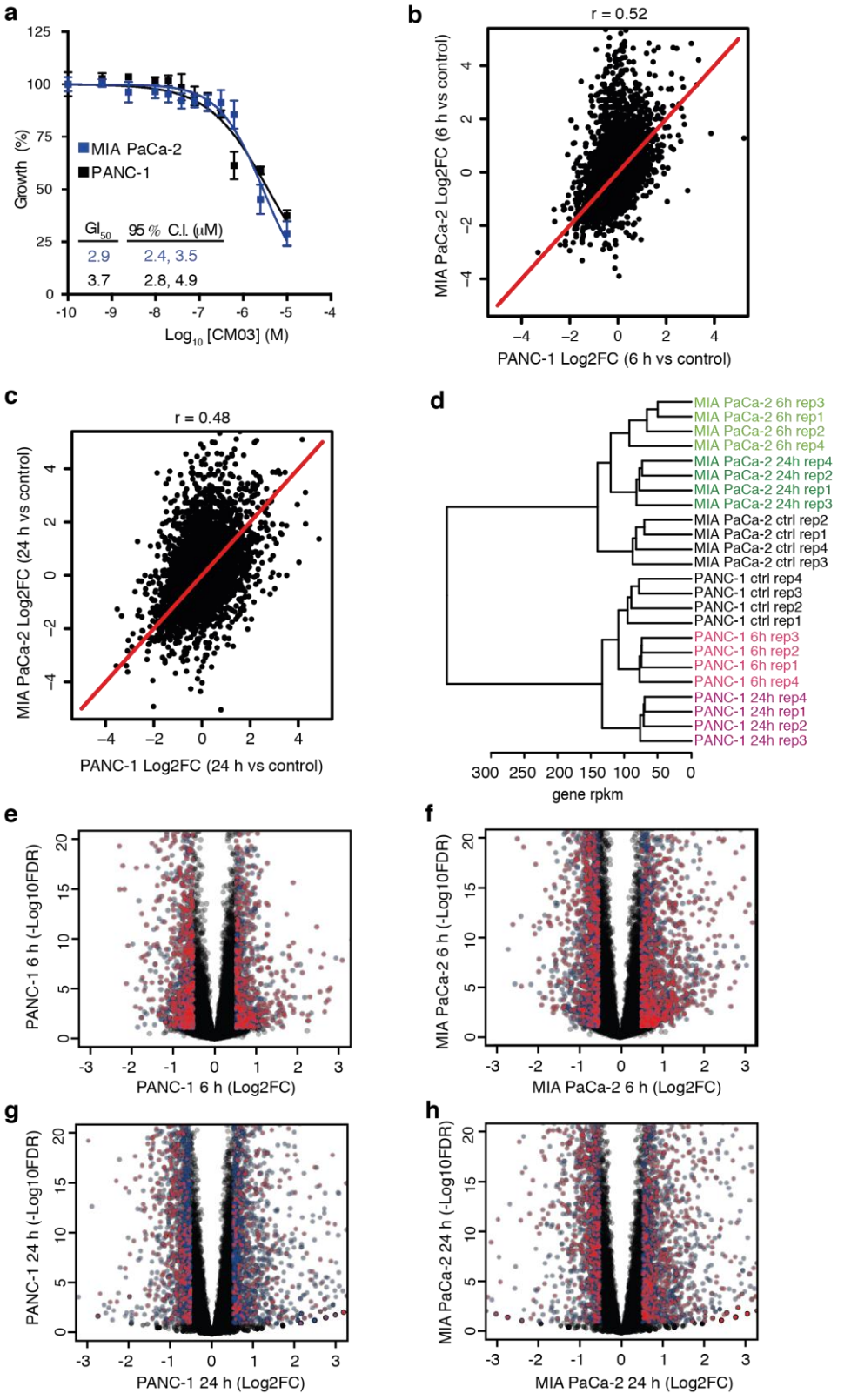
a
Growth (%)
MIA PaCa-2
PANC-1
GI50 95 % C.I. (μM)
2.9 2.4, 3.5
3.7 2.8, 4.9
Log10 [CM03] (M)
b
r = 0.52
MIA PaCa-2 Log2FC (6 h vs control)
PANC-1 Log2FC (6 h vs control)
c
r = 0.48
MIA PaCa-2 Log2FC (24 h vs control)
PANC-1 Log2FC (24 h vs control)
d
MIA PaCa-2 6h rep3
MIA PaCa-2 6h rep1
MIA PaCa-2 6h rep2
MIA PaCa-2 6h rep4
MIA PaCa-2 24h rep4
MIA PaCa-2 24h rep2
MIA PaCa-2 24h rep1
MIA PaCa-2 24h rep3
MIA PaCa-2 ctrl rep2
MIA PaCa-2 ctrl rep1
MIA PaCa-2 ctrl rep4
MIA PaCa-2 ctrl rep3
PANC-1 ctrl rep4
PANC-1 ctrl rep3
PANC-1 ctrl rep2
PANC-1 ctrl rep1
PANC-1 6h rep3
PANC-1 6h rep2
PANC-1 6h rep1
PANC-1 6h rep4
PANC-1 24h rep4
PANC-1 24h rep1
PANC-1 24h rep2
PANC-1 24h rep3
gene rpkm
e
PANC-1 6 h (-Log10FDR)
PANC-1 6 h (Log2FC)
f
MIA PaCa-2 6 h (-Log10FDR)
MIA PaCa-2 6 h (Log2FC)
g
PANC-1 24 h (-Log10FDR)
PANC-1 24 h (Log2FC)
h
MIA PaCa-2 24 h (-Log10FDR)
MIA PaCa-2 24 h (Log2FC)

Supplementary Data Figure 1: The differential gene expression after CM03 treatment is well correlated between PANC-1 and MIA PaCa-2. a) Growth inhibition response curves for PANC-1 and MIA PACA-2 cell lines treated with CM03. Cells were treated for 24 h with a range of CM03 concentrations and cell viability was measured using the CellTiter-Glo Luminescent Cell Viability assay. The concentration causing 50% growth inhibition (GI_{50}) is shown. Results represent the mean and standard deviation from four replicates and are expressed as the percent of viable cells compared with untreated control. The blue and black lines represent MIA PaCa-2 and PANC-1 cell lines, respectively. GI_{50} values with 95 % confidence intervals (95% C.I.) were calculated using GraphPad Prism software using the sigmoidal dose-response (variable slope) equation. **b)** and **c)** Scatter plot indicating the correlation of differential gene expression obtained after treatment of PANC-1 and MIA PaCa-2 cell lines with 400 nM CM03 after (b) 6, and (c) 24 h. Log_2FC is the log2 of the fold change in treatment (6 or 24 h) versus control. 13,044 commonly expressed genes were shared between PANC-1 and MIA PaCa-2 cells over both time points. Red lines show the diagonal. **d)** Hierarchical clustering analysis of differentially expressed genes following 400 nM CM03 treatment. **e)** to **h)** Volcano plots showing transcriptional changes in (e-g) PANC-1 and (f-h) MIA PaCa-2 after 6 and 24 h 400 nM CM03 treatment, respectively. The x-axis represents the –Log10 of the FDR and the x-axis represents the Log2 differential expression for each gene. Blue dots indicate the significant differentially expressed genes (Log_2FC < or >0.5, FDR < 0.1) in the cell line of interest (e.g. PANC-1 in e and g) while the purple dots indicate significant differentially expressed genes of the alternate cell line (e.g. MIA PaCa-2 in e and g) for that time point.

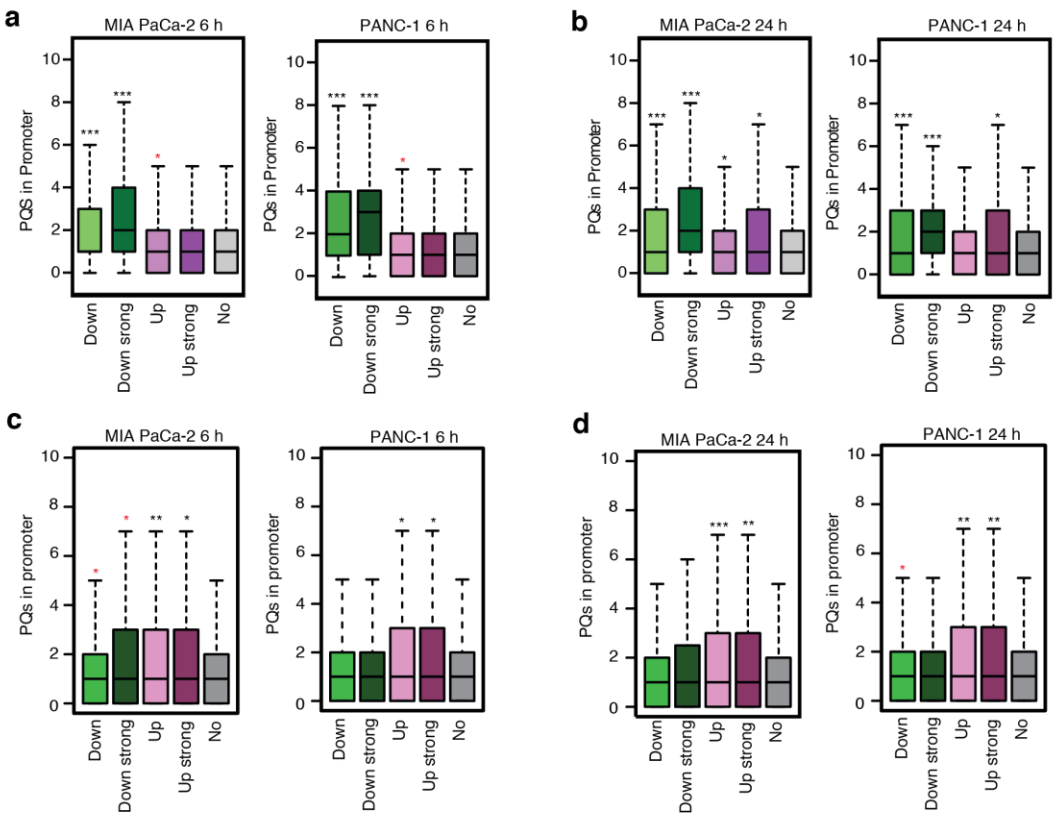

Supplementary Data Figure 2: Differentially down-regulated genes are enriched in promoter PQs in both MIA PaCa-2 and PANC-1 cell lines treated with CM03. MIA PaCa-2 and PANC-1 were treated with **a)** and **b)** 400 nM CM03 and **c)** and **d)** 300 nM gemcitabine for 6 and 24 h and mRNA extracted for analysis via RNA-Seq. Genes were split into four subgroups according to their fold change upon drug treatment versus untreated: Down ($Log_2FC < 0.5$, FDR < 0.1), Up ($Log_2FC > 0.5$, FDR < 0.1), Down strong ($Log_2FC \leq 1.0$, FDR < 0.05) and Up strong ($Log_2FC \geq 1.0$, FDR < 0.05) and analysed for the occurrence of PQs in promoters. Significance between differentially de-regulated gene sets was calculated using the Wilcoxon statistical test via R software. *p < 0.05 and ** p < 1E-10, *** p < 1E-25. Mean number of PQs is significantly lower (red asterisks) or higher (black asterisks) than the gene group with no differential expression (No).

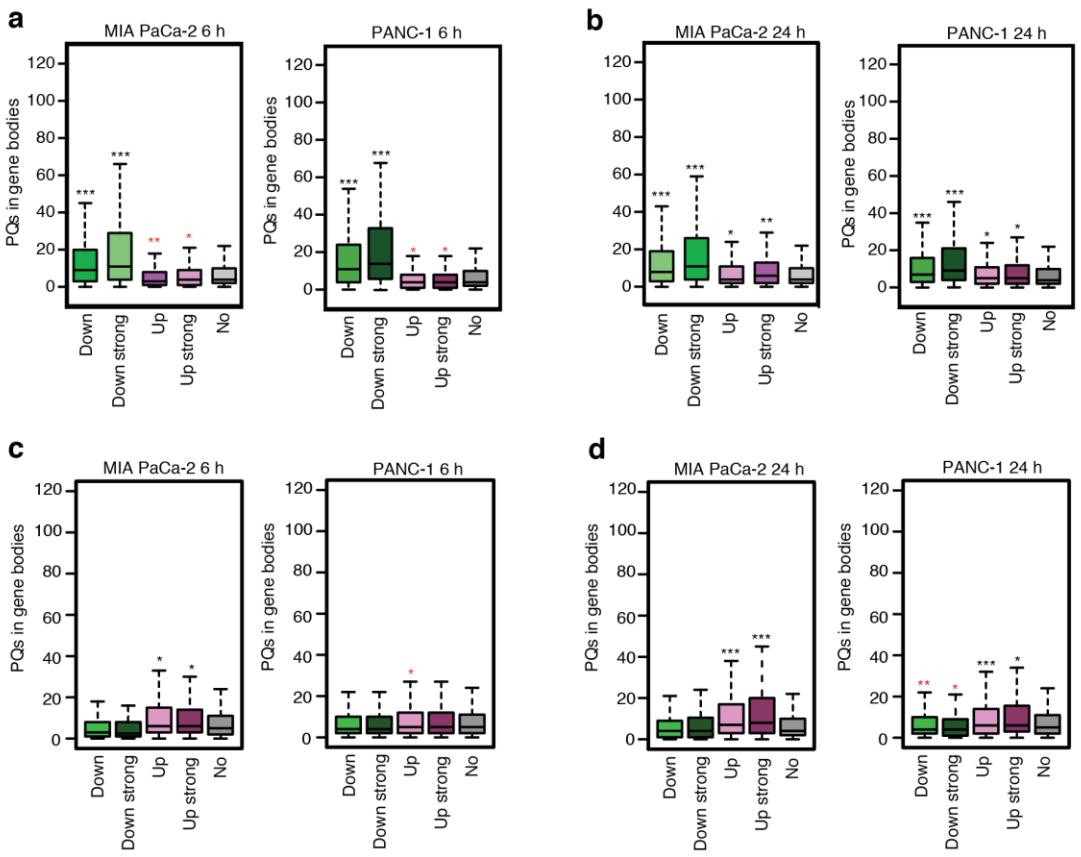

Supplementary Data Figure 3: Differential down-regulated genes are enriched in gene body PQs in both MIA PaCa-2 and PANC-1 cell lines treated with CM03. MIA PaCa-2 and PANC-1 cells were treated with **a)** and **b)** 400 nM CM03 and **c)** and **d)** 300 nM gemcitabine for 6 and 24 h and mRNA extracted for analysis via RNA-Seq. Genes were split into four subgroups according to their fold change upon drug treatment versus untreated as previously described in Supplementary Data Figure 3. Differentially expressed gene sets were analysed for the occurrence of PQs in gene bodies (intron and exons). Significance between differentially de-regulated gene sets was calculated using the Wilcoxon statistical test via R software. *$p < 0.05$ and ** $p < 1E\text{-}10$, *** $p < 1E\text{-}25$. Mean number of PQs is significantly lower (red asterisks) or higher (black asterisks) than the gene group with no differential expression (No).

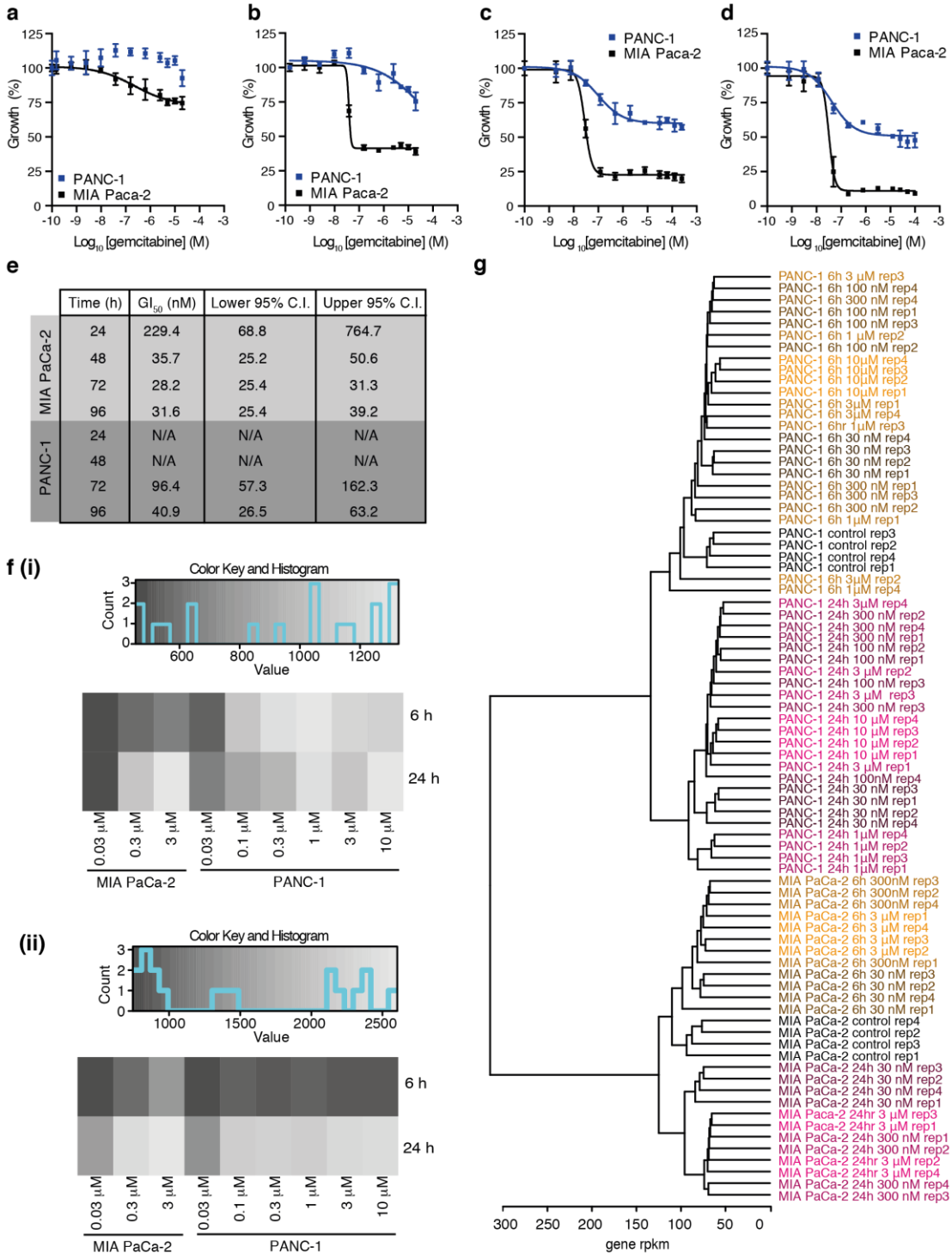

Supplementary Data Figure 4: Summary of RNA-Seq results after gemcitabine treatment in PANC-1 and MIA PaCa-2 cell lines. a) to **e)** Growth inhibition response curves for PANC-1 and MIA PaCa-2 cell lines treated with gemcitabine after (a) 24, (b) 48, (c) 72 and (d) 96 h. (PANC-1 cells are more resistant to gemcitabine treatment than MIA PACA-2[1]). Cell viability was measured using the CellTiter-Glo Luminescent Cell Viability assay and the concentration causing (e) 50% growth inhibition (GI_{50}) was calculated**.** Results represent the mean and 95 % confidence intervals (C.I.) from four replicates and are expressed as percent of viable cells compared with untreated control. The blue and black lines represent

MIA PaCa-2 and PANC-1 cell lines, respectively. GI_{50} values were calculated using GraphPad Prism software using the sigmoidal dose-response (variable slope) equation. **g)** Hierarchical clustering analysis of differentially expressed genes following gemcitabine treatment. Samples are split into two major groups according to cell type, then by treatment time (6 or 24 h) and further into smaller cluster by gemcitabine concentration. **f)** Heat map of (i) down ($Log_2FC < 0.5$, FDR < 0.1), and (ii) up ($Log_2FC > 0.5$, FDR < 0.1), differential expressed genes after gemcitabine treatment for 6 and 24 h at indicated concentrations. Lighter colours indicate greater numbers of de-regulated genes, as detailed in the colour key and histogram insets: MIA PaCa-2 cells show increasing response with dose and treatment time for both up- and down-regulated genes, whilst PANC-1 cells show little response to concentration. MIA PaCa-2 cells show better separation than PANC-1 by concentration, similar to what is shown in (f), reflecting PANC-1 resistance to gemcitabine.

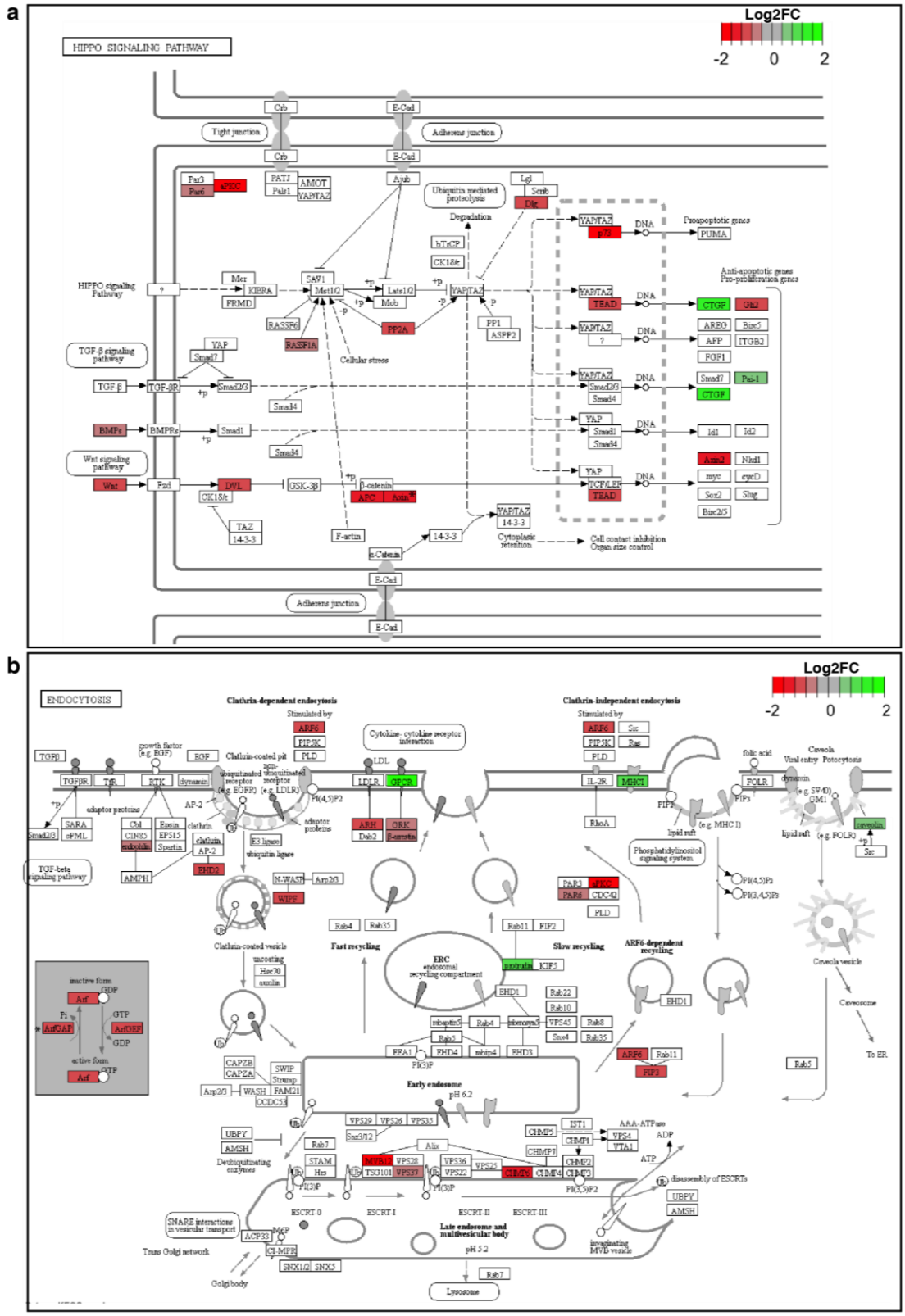
a
Log2FC
-2
0
2
HIPPO SIGNALING PATHWAY
Crb
E-Cad
Tight junction
Adherens junction
PATJ
AMOT
YAP/TAZ
Ajub
Ubiquitin mediated proteolysis
Lgl
Scrib
Dlg
Degradation
bTrCP
CK1δ/ε
YAP/TAZ
p73
DNA
Proapoptotic genes
PUMA
HIPPO signaling Pathway
Mer
KIBRA
FRMD
SAV1
Mst1/2
Lats1/2
Mob
YAP/TAZ
TEAD
CTGF
Gli2
Anti-apoptotic genes
Pro-proliferation genes
AREG
Bcre5
AFP
ITGB2
FGF1
RASSF6
RASSF1A
PP2A
FP1
ASPP2
Cellular stress
TGF-β signaling pathway
YAP
Smad7
TGF-β
TGF-βR
Smad2/3
Smad4
Smad7
Pai-1
CTGF
BMPs
BMPRs
Smad1
Id1
Id2
Wnt signaling pathway
Wnt
Fzd
DVL
GSK-3β
β-catenin
APC
Axin
CK1δ/ε
TCF/LEF
Axin2
Nkd1
myc
cyclD
Sox2
Slug
Bmc2/5
TAZ
14-3-3
F-actin
β-Catenin
Cytoplasmic retention
Cell contact inhibition
Organ size control
b
Log2FC
-2
0
2
ENDOCYTOSIS
Clathrin-dependent endocytosis
Stimulated by
Clathrin-independent endocytosis
Cytokine- cytokine receptor interaction
TGFβ
growth factor (e.g. EGF)
EGF
TGFβR
TβR
RTK
dynamin
Clathrin-coated pit
ubiquitinated receptor (e.g. EGFR)
non-ubiquitinated receptor (e.g. LDLR)
LDL
LDLR
CIECR
IL-2R
MHCI
folic acid
FOLR
Caveola
Viral entry
Potocytosis
dynamin
(e.g. SV40)
GM1
lipid raft
(e.g. MHC I)
(e.g. FOLR)
caveolin
Src
adaptor proteins
AP-2
PI(4,5)P2
PIP5
SARA
cPML
Cbl
CIN85
endophilin
Eps15
Epsin
Sprotin
clathrin
AP-2
E3 ligase
ubiquitin ligase
ARH
Dab2
ORK
E-caveolin
RhoA
Phosphatidylinositol signaling system
PI(4,5)P2
PI(3,4,5)P3
TGF-beta signaling pathway
AMPH
EHD2
N-WASP
Arp2/3
WIPF
PAR3
PAR6
aPKC
CDC42
PLD
Clathrin-coated vesicle
uncoating
Hsc70
auxilin
Rab4
Rab35
Fast recycling
Rab11
FIP2
Slow recycling
ARF6 dependent recycling
ERC
endosomal recycling compartment
kinesin
KIF5
EHD1
Rab22
Rab10
rabaptin5
Rab5
rabenosyn5
VPS45
Rab8
Snx4
Rab35
EEA1
EHD4
rabip4
EHD3
PI(3)P
ARF6
Rab11
FIP3
Caveola vesicle
Caveosome
To ER
Rab5
inactive form
GDP
Arf
Pi
ArfGAP
GTP
ArfGEF
GDP
active form
GTP
Arf
CAPZB
CAPZA
SWIP
Strumpf
Arp2/3
WASH
FAM21
CODC53
Early endosome
pH 6.2
UBPY
AMSH
Deubiquitinating enzymes
VPS29
VPS26
VPS35
Snx3/12
Rab7
Alix
STAM
Hrs
MVB12
TSG101
VPS28
VPS37
VPS36
VPS22
VPS25
CHMP6
CHMP4
CHMP5
CHMP1
CHMP7
IST1
VPS4
VTA1
CHMP2
CHMP3
AAA-ATPase
ADP
ATP
PI(3)P
PI(3,5)P2
disassembly of ESCRTs
UBPY
AMSH
SNARE interactions in vesicular transport
ESCRT-0
ESCRT-I
ESCRT-II
ESCRT-III
Late endosome and multivesicular body
pH 5.2
invaginating MVB vesicle
ACP33
M6P
CI-MPR
Trans Golgi network
SNX1/2
SNX3
Golgi body
Rab7
Lysosome

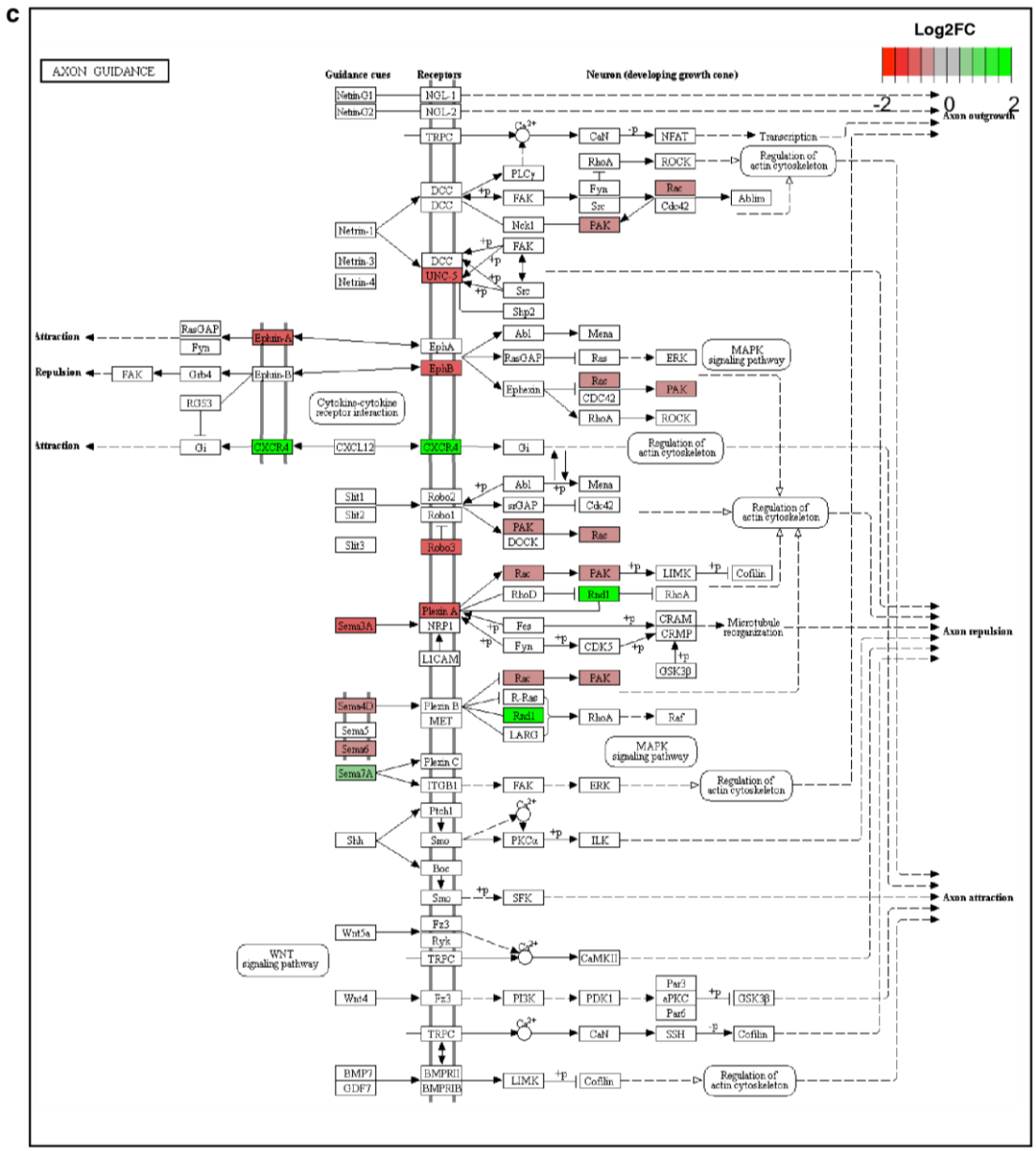

Supplementary Data Figure 5: Significant KEGG pathways for common down-regulated gene set after 6 h CM03 treatment. KEGG pathways showing significantly differentially expressed genes (Log2FC > or < 0.5 and FDR <0.01) for **a)** axon guidance, **b)** hippo signalling and **c)** endocytosis pathways. Genes were rendered in colour indicative of the mRNA fold changes on top of the pathway diagrams. Red: 2-0.5 down-regulation, grey: less than 0.5 fold alteration and green: 0.5-2 fold up-regulation. Any changes with Log2FC > 2 or < 2 are same colour as Log2FC 2. Any gene groups containing both differentially up- and down-regulated genes are marked an asterisk (*)

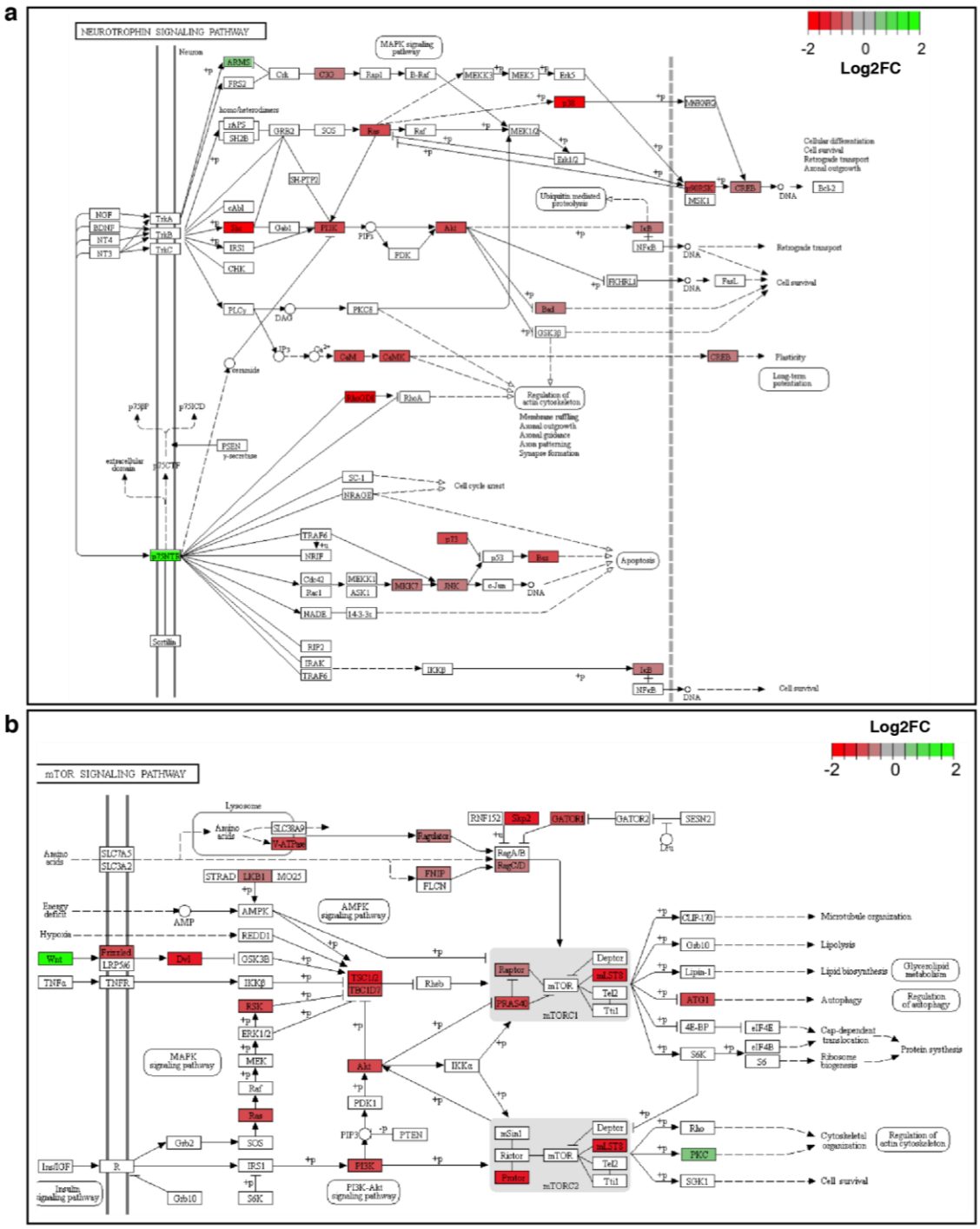
a
NEUROTROPHIN SIGNALING PATHWAY
Log2FC
-2
0
2
b
mTOR SIGNALING PATHWAY
Log2FC
-2
0
2

c

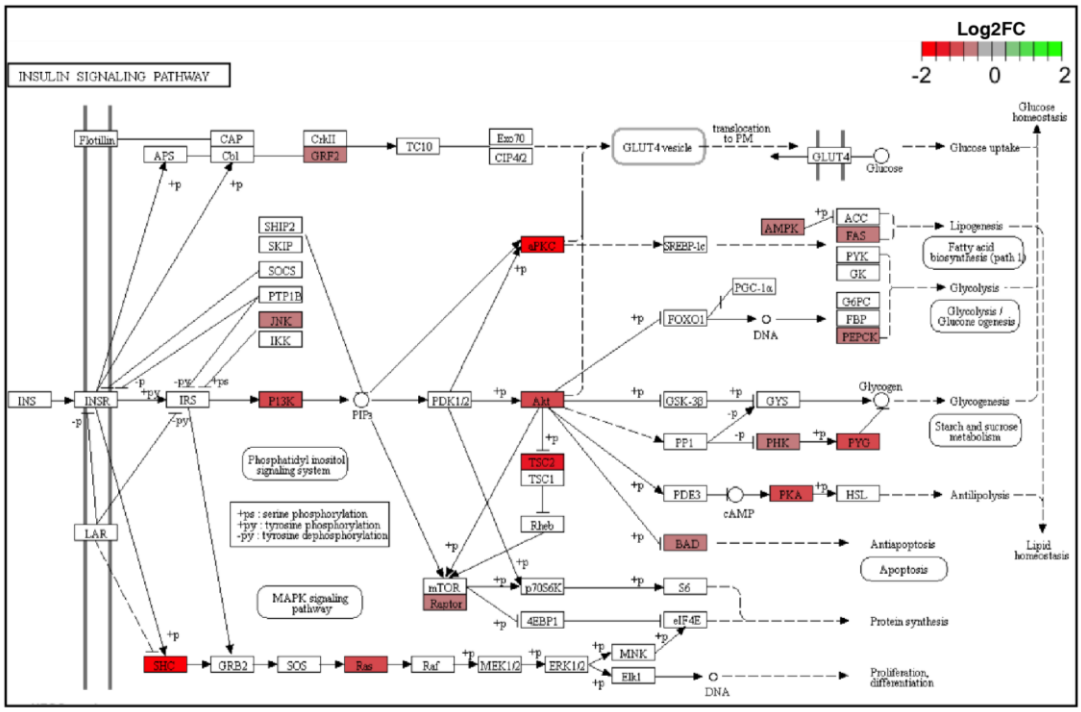
Log2FC
-2
0
2
INSULIN SIGNALING PATHWAY
Flotillin
CAP
Cbl
APS
CrkII
GRB2
TC10
Exo70
CIP4/2
GLUT4vesicle
translocation to PM
GLUT4
Glucose
Glucose uptake
Glucose homeostasis
SHIP2
SKIP
SOCS
PTP1B
JNK
IKK
aPKC
SREBP-1c
AMPK
ACC
FAS
Lipogenesis
Fatty acid biosynthesis (path 1)
PYK
GK
Glycolysis
PGC-1α
FOXO1
DNA
G6PC
FBP
PEPCK
Glycolysis / Gluconeogenesis
INS
INSR
IRS
PI3K
PIPs
PDK1/2
Akt
GSK-3β
GYS
Glycogen
Glycogenesis
Starch and sucrose metabolism
PP1
PHK
PYG
Phosphatidyl inositol signaling system
TSC2
TSC1
Rheb
+ps : serine phosphorylation
+py : tyrosine phosphorylation
-py : tyrosine dephosphorylation
PDE3
cAMP
PKA
HSL
Antilipolysis
LAR
BAD
Antiapoptosis
Apoptosis
Lipid homeostasis
MAPK signaling pathway
mTOR
Raptor
p70S6K
S6
4EBP1
eIF4E
Protein synthesis
SHC
GRB2
SOS
Ras
Raf
MEK1/2
ERK1/2
MNK
Elk1
DNA
Proliferation, differentiation

d

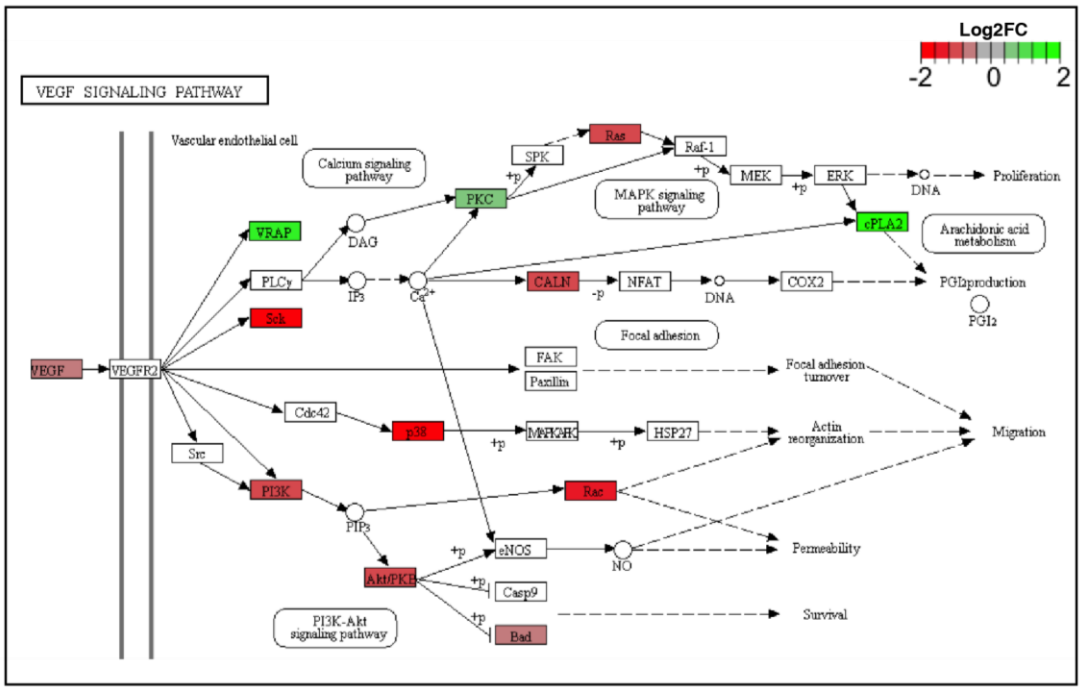
Log2FC
-2
0
2
VEGF SIGNALING PATHWAY
Vascular endothelial cell
Calcium signaling pathway
SPK
Ras
Raf-1
MEK
ERK
Proliferation
DNA
PKC
MAPK signaling pathway
VRAP
DAG
cPLA2
Arachidonic acid metabolism
PLCγ
IP3
Ca2+
CALN
NFAT
DNA
COX2
PGI2production
PGI2
Sck
Focal adhesion
VEGF
VEGFR2
FAK
Paxilin
Focal adhesion turnover
Cdc42
p38
MAPKAPK
HSP27
Actin reorganization
Migration
Src
PI3K
Rac
PIPs
eNOS
NO
Permeability
Akt/PKB
Casp9
Bad
Survival
PI3K-Akt signaling pathway

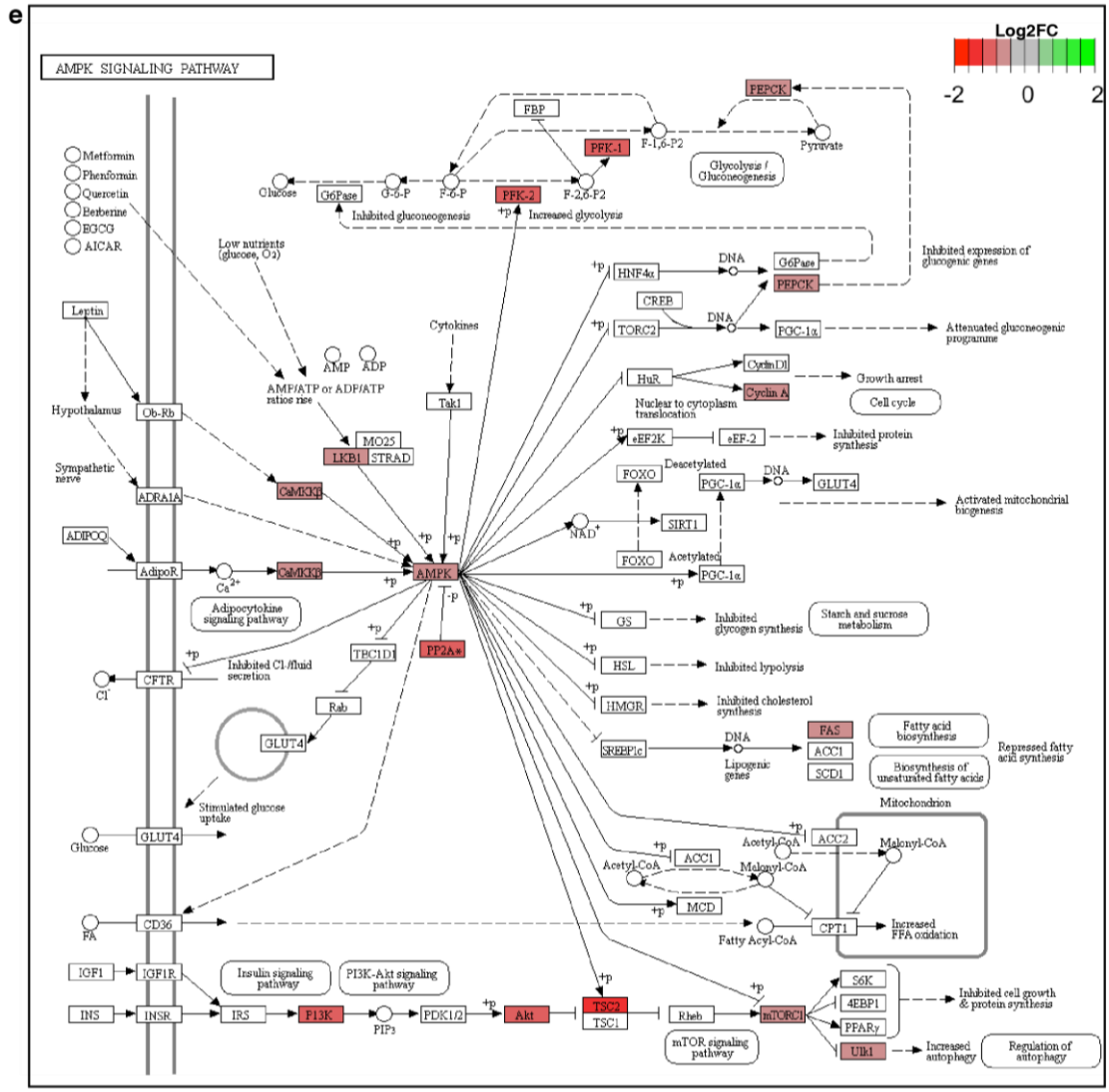

Supplementary Data Figure 6: KEGG pathway diagrams for significant common down-regulated gene set after 24 h CM03 treatment. KEGG pathways showing significantly differentially expressed genes (Log2FC > or < 0.5 and FDR <0.01) for the **a)** neurotrophin, **b)** mTOR**, c)** insulin**, d)** VEGF and **e)** AMPK signalling pathways. Genes were rendered in colour indicative of the mRNA fold changes on top of the pathway diagrams. Red: 2-0.5 down-regulation, grey: less than 0.5 fold alteration and green: 0.5-2 fold up-regulation. Any changes with Log2FC > 2 or < 2 are same colour as Log2FC 2. Any gene groups containing both differentially up- and down-regulated genes are marked an asterisk (*)

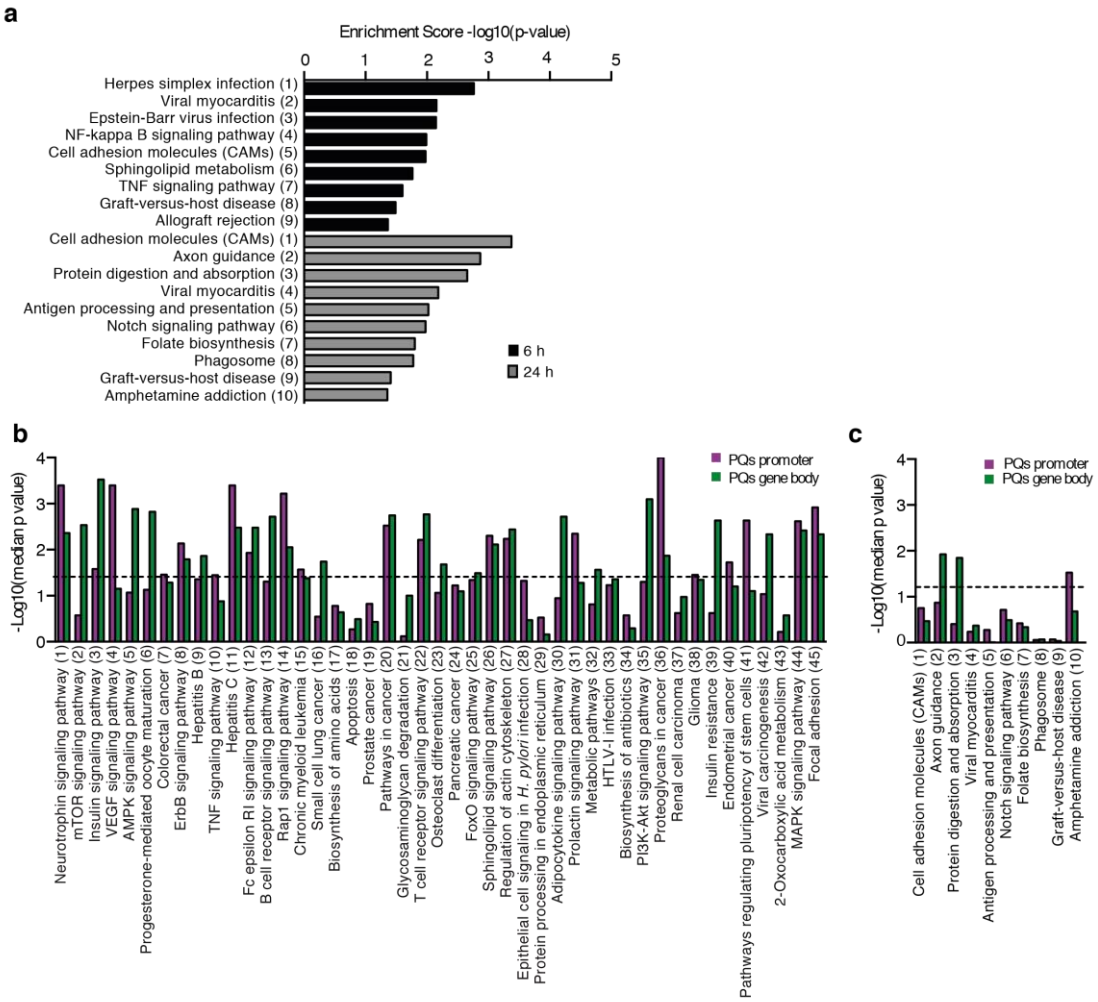

Supplementary Data Figure 7: Graphs of enriched KEGG pathways for common up-regulated genes after CM03 treatment and promoter and gene body PQs analysis for enriched KEGG pathways after 24 h CM03 treatment. a) Enriched KEGG pathways (p-EASE ≤ 0.05) of up-regulated genes ($Log_2FC > 0.5$, FDR < 0.1) common to both PANC-1 and MIA PaCa-2 cell lines after 6 and 24 h 400 nM CM03 treatment. **b)** and **c)** Promoter and gene body PQs analysis of (b) down- and (c) up-regulated enriched KEGG pathways after 24 h 400 nM CM03 treatment. PQs analysis for each enriched KEGG pathways were performed as previously described. Note the increased number of KEGG pathways crossing the significant PQs enrichment threshold (represented by the dotted line) for down-regulated genes (b) compared to (c).

Extended Methods – RNA-Seq

For the putative G4 sequences (PQs) analysis, the occurrence of the canonical G4 motif ($G_{\geq 3}N_{1\text{-}7}G_{\geq 3+}N_{1\text{-}7}G_{3\geq}N_{1\text{-}7}G_{\geq 3}$), as previously defined[2,3], was calculated both in gene promoters (defined as 2 kilobases upstream of the transcription start site (TSS) and 100 bases downstream) and gene bodies (exons and introns). Genes were split into different subsets according to their fold changes for drug treatment versus untreated, with the following assignment: Down Strong = genes with Log-fold change (Log_2FC) ≤ -1 and false discovery rate (FDR) < 0.05; Down = genes with Log_2FC < -0.5 and FDR < 0.1; Strong Up = genes with Log_2FC ≥ 1 and FDR < 0.05; Up = genes with Log_2FC > 0.5 and FDR < 0.1; NO = genes not differentially expressed, i.e. not present in any of the previous categories. The KEGG pathway enrichment analysis was done using the DAVID functional annotation tool (https://david.ncifcrf.gov/)[4] on the Up and Down gene lists, for the MIA PaCa-2 and PANC-1 differentially expressed genes individually and for the common genes. The open source software Cytoscape 3.5.1[5] and Cytoscape ClueGO app[6] were used to visualise networks of the associated KEGG pathways. The PQs analysis within the enriched pathways was implemented as follows: for each pathway enriched (p-EASE ≤ 0.05) and for each gene list, the number of PQs in promoter regions (or gene bodies) was counted, and a random distribution was generated by sampling 10,000 times gene sets of the same size of the gene subset in the given pathway. The p-value was empirically estimated from there as the number of times the random count was higher or equal to the PQs count in promoter (or gene bodies), divided by the number of randomizations (10,000). Data on the KEGG pathway graphs were rendered using the R/Bioconductor package Pathview[7].

For gemcitabine RNA-seq data, the analysis was performed identically to the CM03 libraries, but the two cell lines were independently analyzed. The PQs analysis in promoters and gene bodies and functional annotation was performed as described for CM03.

Extended Methods – immunofluorescence

BG4 and 53BP1 foci quantification and colocalization analysis was performed automatically in 3D using a custom protocol in the open source imaging software ICY (http://icybioimageanalysis.org)[8]. The ICY protocol is provided in the supplementary file (ICY_BG4_53BP1_coloc_final.protocol) at https://github.com/JeremyPike/ColocalizationStudio-modified/ and all parameters are as specified. This file can be directly opened by the free open-source software that can be downloaded from the website. The modified colocalisation plugin required for the ICY protocol is available at https://github.com/JeremyPike/ColocalizationStudio-modified/. First, spot-like features were detected in the BG4 and 53BP1 channels using an un-decimated wavelet transform[9]. Nuclear regions were segmented from the

DAPI channel using a hierarchical K-means clustering algorithm with ten intensity classes[10]. For each nuclear region the corresponding BG4 and 53BP1 features were counted and an object based co-localisation analysis based on the Ripley K-function was performed[11,12]. Specifically the number of BG4 foci, 53BP1 foci and BG4-53BP1 co-localisations and percentage of BG4-53BP1 co-localisations per nucleus were calculated.

References:

1. Fryer, R. A.; Barlett, B.; Galustian, C.; Dalgleish, A. G. Mechanisms underlying gemcitabine resistance in pancreatic cancer and sensitisation by the iMiD lenalidomide. *Anticancer Res.* **2011**, *31*, 3747-3756.
2. Todd, A. K.; Johnston, M.; Neidle, S. Highly prevalent putative quadruplex sequence motifs in human DNA. *Nucleic Acids Res.* **2005**, *33*, 2901-2907.
3. Huppert, J. L.; Balasubramanian, S. Prevalence of quadruplexes in the human genome. *Nucleic Acids Res.* **2005**, *33*, 2908-2916.
4. Huang, D. W.; Sherman, B. T.; Lempicki, R. A. Systematic and integrative analysis of large gene lists using DAVID bioinformatics resources. *Nat. Protocols* **2008**, *4*, 44-57.
5. Shannon, P.; Markiel, A.; Ozier, O.; Baliga, N. S.; Wang, J. T.; Ramage, D.; Amin, N.; Schwikowski, B.; Ideker, T. Cytoscape: a software environment for integrated models of biomolecular interaction networks. *Genome Res.* **2003**, *13*, 2498-2504.
6. Bindea, G.; Mlecnik, B.; Hackl, H.; Charoentong, P.; Tosolini, M.; Kirilovsky, A.; Fridman W. H.; Pagès, F.; Trajanoski, Z.; Galon, J. ClueGO: a Cytoscape plug-in to decipher functionally grouped gene ontology and pathway annotation networks. *Bioinformatics* **2009**, *25*, 1091-1093.
7. Luo, W.; Pant, G.; Bhavnasi, Y. K.; Blanchard, S. G. Jr.; Brouwer, C. Pathview Web: user friendly pathway visualization and data integration. *Nucleic Acids Res*. **2017**, doi: 10.1093/nar/gkx372
8. de Chaumont, F.; Dallongeville, S.; Chenouard, N.; Hervé, N.; Pop, S.; Provoost, T.; Meas-Yedid, V.; Pankajakshan, P.; Lecomte, T.; Le Montagner, Y.; Lagache, T.; Dufour A.; Olivo-Marin, J.-C. Icy: an open bioimage informatics platform for extended reproducible research. *Nat. Methods* **2012**, *9*, 690-696.
9. Olivo-Marin, J.-C. Extraction of spots in biological images using multiscale products. *Pattern Recogn.* **2002**, *35*, 1989-1996.
10. Dufour, A.; Meas-Yedid, V.; Grassart, A.; Olivo-Marin, J.-C. Automated quantification of cell endocytosis using active contours and wavelets. in *2008 19th Intern. Confer. Pattern Recogn.* **2008**, 1-4.
11. Lagache, T.; Meas-Yedid, V.;Olivo-Marin, J.-C. A statistical analysis of spatial colocalization using Ripley's K function. in *2013 IEEE 10th Internat. Symp. Biomed. Imaging* **2013**, 896-901.
12. Lagache, T.; Sauvonnet, N.; Danglot, L.; Olivo-Marin, J.-C. Statistical analysis of molecule colocalization in bioimaging. *Cytometry. Pt. A: J. Intern. Soc. Anal. Cytol.* **2015**, *87*, 568-579.

Supporting Tables

Supporting Table 1: Deregulated genes upon 400 nM CM03 treatment

Description: Processed RNA-seq data for PANC-1 and MIA PaCa-2 containing gene log fold changes upon 6 and 24 h 400 nM CM03 treatment compared to control. Genes are grouped into four categories Down Strong, Up strong, Down and Up as per methods. The number of PQs found in the gene body (exon and introns) and promoter region (both strands or same strand as TSS) for each gene is also stated.

Supporting Table 2: Common deregulated genes upon 400 nM CM03 treatment.xlsx

Description: Processed RNA-seq data for genes in common between PANC-1 and MIA PaCa-2 upon 6 and 24 h 400 nM CM03 treatment. Genes are grouped into four categories Down Strong, Up strong, Down and Up as per methods. The number of PQs found in the gene body (exon and introns) and promoter region (both strands or same strand as TSS) for each gene is also stated.

Supporting Table 3: Statistics for PQs box and whisker plots.xls

Description: Table contains the median, mean, 25% percentile, 75% percentile, maximum, minimum values, p-value (calculated from Wilcox test), gene summary and ratio of the means for each of the box and whisker plots from Figures 3a,b and Supporting Information Figures 2 and 3.

Supporting Table 4: Deregulated genes upon 300 nM gemcitabine treatment.xls

Description: Processed RNA-seq data for PANC-1 and MIA PaCa-2 containing gene log fold changes upon 6 and 24 h 300 nM gemcitabine treatment compared to control. Genes are grouped into four categories Down Strong, Up strong, Down and Up as per methods. The number of PQs found in the gene body (exon and introns) and promoter region (both strands or same strand as TSS) for each gene is also stated.

Supporting Table 5: KEGG pathways of common differentially deregulated genes upon 400 nM CM03 treatment.xls

Description: KEGG pathways and associated genes for the up and down differentially expressed genes found in common between PANC-1 and MIA PaCa-2 after 6 and 24 h CM03 treatment.

Supporting Table 6: KEGG pathways of differentially deregulated genes upon 400 nM CM03 treatment.xls

Description: KEGG pathways and associated genes for the up and down differentially expressed genes for PANC-1 and MIA PaCa-2 (analyzed individually) after 6 and 24 h 400 nM CM03 treatment.

Supporting Table 7: KEGG pathways of differential deregulated genes upon 300 nM gemcitabine treatment.xlsx

Description: KEGG pathways and associated genes for the up and down differentially expressed genes for PANC-1 and MIA PaCa-2 (analyzed individually) after 6 and 24 h 300 nM gemcitabine treatment.